



Determination of Lead and Chromium in Aloe Vera Pulp and Aloe Vera-Based Cosmetics by Laser-Induced Breakdown Spectroscopy (LIBS)

Imran Rehan, Muhammad Zubair Khan, Kamran Rehan, Sabiha Sultana, Irfan Qasim, Salah Ud Din, Hafeez Anwar & Sayyar Muhammad

To cite this article: Imran Rehan, Muhammad Zubair Khan, Kamran Rehan, Sabiha Sultana, Irfan Qasim, Salah Ud Din, Hafeez Anwar & Sayyar Muhammad (2020): Determination of Lead and Chromium in Aloe Vera Pulp and Aloe Vera-Based Cosmetics by Laser-Induced Breakdown Spectroscopy (LIBS), Analytical Letters

To link to this article: <https://doi.org/10.1080/00032719.2020.1748044>



Published online: 16 Apr 2020.



Submit your article to this journal [↗](#)



View related articles [↗](#)



View Crossmark data [↗](#)



Determination of Lead and Chromium in Aloe Vera Pulp and Aloe Vera-Based Cosmetics by Laser-Induced Breakdown Spectroscopy (LIBS)

Imran Rehan^a, Muhammad Zubair Khan^b, Kamran Rehan^c, Sabiha Sultana^d, Irfan Qasim^e, Salah Ud Din^f, Hafeez Anwar^g, and Sayyar Muhammad^d

^aDepartment of Physics, Islamia College University, Peshawar, Pakistan; ^bDepartment of Applied Physics, Federal Urdu University of Arts, Science and Technology, Islamabad, Pakistan; ^cState Key Laboratory of Magnetic Resonance and Atomic and Molecular Physics, Wuhan Institute of Physics and Mathematics, Chinese Academy of Sciences, Wuhan, China; ^dDepartment of Chemistry, Islamia College University, Peshawar, Pakistan; ^eDepartment of Physics, Riphah International University, Islamabad; ^fDepartment of Chemistry, University of Azad Jammu and Kashmir, Azad Kashmir, Muzaffarabad, Pakistan; ^gDepartment of Physics, University of Agriculture Faisalabad, Faisalabad, Pakistan

ABSTRACT

This study focuses on the application of laser-induced breakdown spectroscopy (LIBS) to determine lead and chromium in pristine aloe vera and aloe vera based beauty soaps using the second harmonic (532 nm) of a Q-switched Nd:YAG laser. The optimal experimental conditions were evaluated to improve the sensitivity of the detection system by a parametric dependence study. The atomic transition lines at 405.7 nm and 425.4 nm were used as the analytical lines to determine lead and chromium, respectively. The LIBS system was calibrated for these toxic elements and the samples under analysis included 8.00–15.00 ppm by mass of lead and 5.00–12.00 ppm by mass of chromium, which are far above the safe permissible levels of these elements (i.e., 0.50 ppm for Pb and 1.00 ppm for Cr). The quantitative results were checked before and after normalization with the background and better outcomes were obtained when the spectrum was normalized with the background. The LIBS results were compared to the outcomes of selected samples by a standard analytical method, inductively coupled plasma – optical emission spectroscopy (ICP-OES). Both outcomes were in outstanding conformity implying the reliability of the LIBS measurements. The current study is attractive for the general evaluation of human health and specifically for the analysis of aloe vera based cosmetics.

ARTICLE HISTORY

Received 23 November 2019
Accepted 24 March 2020

KEYWORDS

Laser-induced breakdown spectroscopy (LIBS); lead; chromium; aloe vera

Introduction

In recent years, the use of personal care products has enlarged globally. Numerous personal care products including face wash, beauty powders, lipstick, soaps, cream, lotions, shampoo, and body sprays are used extensively in our everyday life. The beauty soap is a facial care product that is normally used to improve the skin complexion and to

CONTACT Imran Rehan  irehanyousafzai@gmail.com  Department of Physics, Islamia College University, Peshawar, 25120 Pakistan.

Imran Rehan and Kamran Rehan contributed equally to this work.

© 2020 Taylor & Francis Group, LLC

remove various types of pollution such as dust, oil, and dirt. The excessive and misleading advertisements of cosmetics provides little information about the actual value of personal care products (Wilding, Curtis, and Welker-Hood 2009).

Regardless of the caring role of skin against external pollutants, several of the ingredients in cosmetic items are able to penetrate into the skin and may cause systemic exposure (Lorentz et al. 2008; Nohynek et al. 2010). According to the National Institute for Occupational Safety and Health (NIOSH), USA, the long-standing and large quantity use of personal care products may be hazardous to human health due to the presence of toxins in the chemicals utilized in personal care products (Lambers et al. 2006). Natural toxins and synthetic ingredients in cosmetics may generate local effects on human skin that include irritation, allergy, or photoreactions (Tomankova et al. 2011).

Amongst the harmful species present in cosmetics, toxic metals such as lead are broadly used in colored makeup products. The ingestion of lead exposes humans to behavioral, physical, reproduction and mental problems along with negative impacts upon the kidneys, red blood cells and bones (Luo et al. 2012; Vige, Saito, and Sawada 2011). Similarly, exposure to Cr above the safe limit may trigger pulmonary congestion, cancer, respiratory irritation, and liver impairment (Baral and Engelken 2002). Skin exposure, inhalation, and ingestion are possible ways for these deadly metals to enter adults while children are at risk through gastrointestinal zones (Al-Saleh 1998). It is alarming that the maximum permissible limits for Pb and Cr are 0.50 and 1.00 ppm, respectively (Renfrew 1991).

Various analytical methods, including inductively coupled plasma – mass spectrometry (Hepp, Mindak, and Cheng 2009), flame atomic absorption spectrometry (Saeed, Muhammad, and Khan 2011), and graphite furnace atomic absorption spectrometry (Al-Saleh, Al-Enazi, and Shinwari 2009) have been used to characterize the chemical composition of cosmetic products. All of these analytical methods involve tedious sample preparation procedures that may affect the actual chemical composition of the sample, particularly for the trace determination of contaminants in samples. Under these conditions, the results may become unreliable.

Laser-induced breakdown spectroscopy (LIBS) is an alternative approach for these analyses (Augusto, Batista, and Pereira-Filho 2016; Gondal et al. 2013; Gondal et al. 2010). LIBS is capable of analyzing samples, irrespective of the physical state, i.e., solid, liquid, gaseous or aqueous phase. This technique only needs a small quantity of sample with almost no sample preparation and may be applied to concurrently determine multiple elements.

LIBS employs a high power laser pulse focused on the target that forms a plasma upon its surface. The spectral signatures of atomic and ionic emissions are observed when plasma cools down. The plasma contains the useful information regarding the elemental composition of sample, which are acquired by an optical assembly and directed to a high resolution spectrometer. The spectral signatures of the acquired spectra may be characterized with the help of the National Institute Standard Technologies (NIST) atomic database and a survey of the literature.

In the current work, the detection system was optimized to improve the sensitivity to determine trace levels of lead and chromium present in pristine aloe vera pulp and aloe vera based beauty soaps accessible in the local market. Due to ethical reasons, the brand

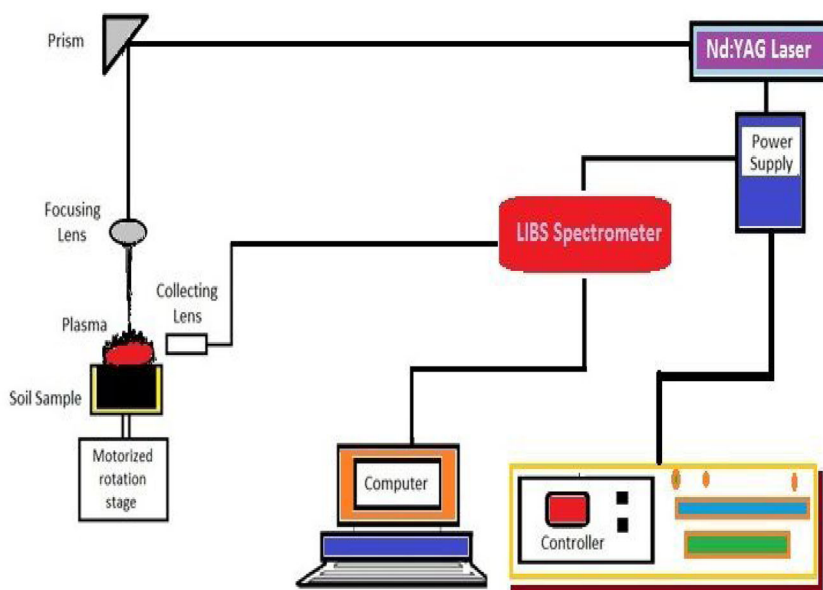


Figure 1. Schematic of the LIBS experimental arrangement.

names of the personal care products were kept anonymous and the samples were labeled with codes. The strong atomic transition lines of lead Pb I at 405.7 nm and chromium Cr I at 425.4 nm were used as the fingerprint atomic transition lines for their identification and quantification. The analytical measurements were performed under conditions forming an optically thin plasma by establishing the assumption of the local thermodynamic equilibrium of the plasma plume (Rehan et al. 2017). The current study is extremely significant for human health, explicitly for people using aloe vera based cosmetics for the beautification of their skin.

Experimental methods

LIBS system

A beam from a Q-switched Nd:YAG laser (Quantel Brilliant) operating at 532 nm with a pulse width of 5 ns and a repetition rate of 10 Hz was employed as the source for excitation. The laser is capable to deliver energy up to 200 mJ/pulse at 532 nm. The plasma plume was formed on the target by focusing a pulsed laser beam onto the surface via a convex lens with 20 cm focal length.

The current experimental setup is depicted as in Figure 1. The sample was placed on an X-Y translator which moved with a uniform speed throughout the laser ablation process to limit surface pitting and the accompanying signal attenuation due to variations in the focal point of the laser beam. The emission from plasma was recorded through a quartz window using the LIBS2000 detector in conjunction with an optical fiber (high OH, core diameter of 600 μm) with a collimating lens having a 0° to 45° field of view. The collected light was subsequently guided to a dedicated high-resolution spectrometer (Ocean Optics, Inc).

A calibrated energy meter was used to monitor the pulsed laser energy through an incorporated capability in the Nd:YAG laser. The LIBS2000 detection system consisted of five high-resolution small miniature spectrometers, each with a slit width of 5 μm , 2048 element linear charge coupled devices, and different groove densities on a grating with 2400 lines/mm and 1800 lines/mm, thereby covering a spectral range from 200 to 700 nm. The data obtained by the five spectrometers were stored on a computer through the instrumental software.

To eliminate the pulse-to-pulse variations in the laser energy, the LIBS measurements were normalized. The normalization was performed through the following shots to obtain the average spectra. The averaged emission spectra were then utilized for subsequent analysis. The emission signals were corrected by subtracting the dark signals using the OOILIBS software.

Sample collection for LIBS analysis

The current analysis was performed to investigate the concentrations of the toxic metals lead and chromium in aloe vera based beauty soaps of various brands. For this intention, three aloe vera based soap samples of various quality, brand and prices were purchased from various cosmetic shops in Pakistan. Pristine aloe vera pulp was also examined similarly for comparative studies. The acquired samples were designated as soap 1 (aloe vera based beauty soap, local), soap 2 (aloe vera based beauty soap, International), soap 3 (aloe vera based beauty soap, International), and pulp (pristine aloe vera pulp, collected locally).

The soap samples were first cut into small pieces and then placed in desiccators in order to completely dry them. The cutting device was washed with distilled water to remove any contamination before cutting. The dried samples were crushed to a fine powder and pressed to pellets by a utilizing stainless steel cylindrical die having a diameter of approximately 20 mm and thickness of approximately 2 mm.

The pellets were then attached to a target holder moving uniformly at a rate of approximately 6.0 mm/s to reduce the erosion of the spot and to irradiate a fresh surface in every laser shot. Similarly, the pristine aloe vera, i.e., the clear pulp which is also known as the inner gel of the aloe vera leaf, was dried in desiccators and was pulverized into a fine powder to transform it in homogeneous pellets.

In order to calibrate the LIBS system, solid stoichiometric samples having various concentrations of lead and chromium equal to 5, 20, 40, 60, and 80 ppm were prepared by the homogeneous mixing of 99.99% pure lead and chromium into the pristine aloe vera pulp and aloe vera based soap sample.

For the ICP-OES analysis of selected samples, each powdered sample was first digested by the addition of nitric acid (HNO_3) and hydrogen peroxide (H_2O_2). The resulting solution was refluxed at approximately 95 $^\circ\text{C}$ for 5 h to complete the exothermic reaction. The solution was then diluted to the desired final volume and analyzed by inductively coupled plasma optical emission spectrometry.

Results and discussion

Determination of the optimum LIBS parameters for sensitive detection

In order to improve the sensitivity of the LIBS system, the experimental setup was optimized for different LIBS parameters including the optimization of the time delay

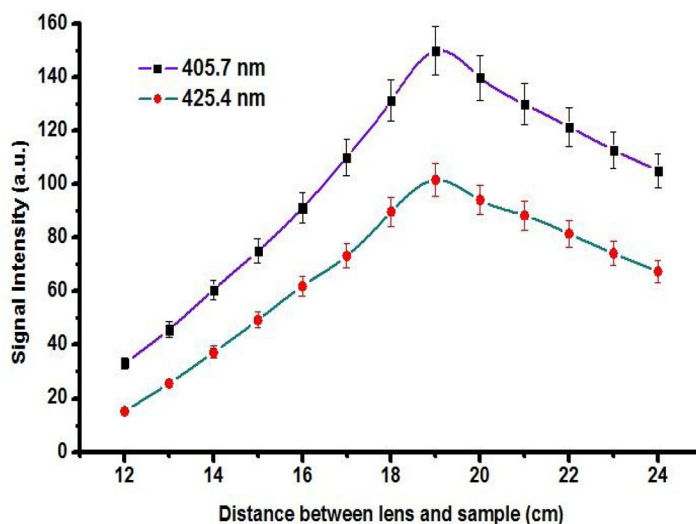


Figure 2. Influence of the separation distance from the lens to the sample by monitoring the LIBS intensity for Pb at 405.7 and Cr at 425.4 nm in the soap 1 sample in air at atmospheric pressure with excitation by Nd:YAG pulses at 532 nm.

between the trigger of laser pulse and the collection of the emission spectrum, the distance between the focusing lens and sample, and the laser irradiance. The distance between the focusing lens and target was optimized by studying the influence of its separation on the quality of spectra. For this study, variable target to lens distances of 12, 13, 14, 15, 16, 17, 18, 19, 20, 21, 22, 23, and 24 cm were employed. The impacts of the distance between lens and sample upon the spectral emission lines for Pb at 405.7 nm and Cr at 425.4 nm are shown in Figure 2.

According to the distribution of the emission intensities, the results show that the optical emission intensities are increased from 12 cm to 19 cm and decrease at longer distances. The maximum signal intensities were observed at a distance of 19 cm between the lens and sample without any saturation. At the initial stages of plasma formation, at times less than 400 ns following excitation, the characteristic LIBS spectrum is primarily continuum background noise resulting from the blackbody radiation of the plasma and elastic collisions of electrons with the non-neutral species (Bremsstrahlung). Simultaneously, weak neutral and broadened ionic peaks are superimposed over the continuum moreover that generally overlap.

After an appropriate time delay, the generated plasma expands and cools, thereby emitting well-defined distinguishing spectral transitions of atomic as well as ionized species present in the target (Harilal et al. 1998). Hence, the time delay between the trigger of the laser pulse and collection of the spectrum must be optimized to reduce the background noise and increase the intensity of the spectral line of interest. The optimum delay time was determined by recording the integrated signal intensity at various time delays for the fingerprint wavelengths for Pb I at 405.7 nm and Cr I at 425.4 nm. The optimization of time delay was considered across a wide range of intervals from 300 to 1100 ns for Pb I at 405.7 nm and 300 to 1100 ns for Cr I at 425.4 nm. The period between each time delay interval was 200 ns for both elements.

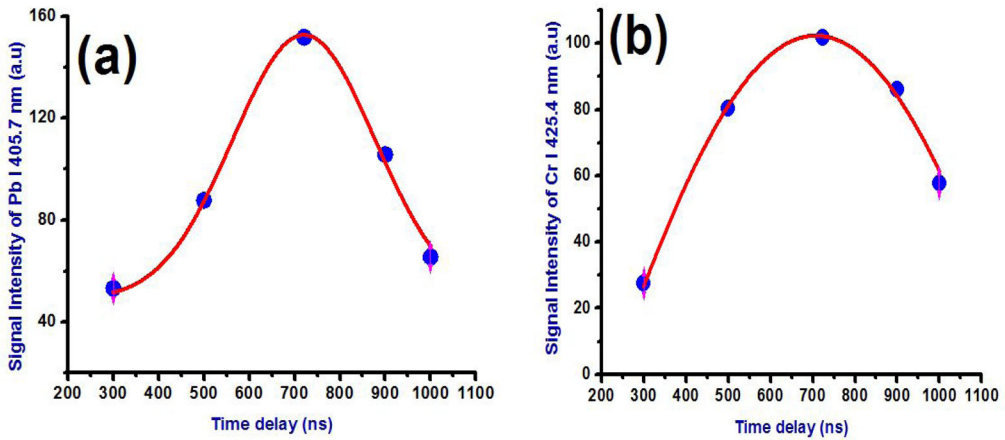


Figure 3. Influence of the time delay upon the LIBS intensity for: (a) Pb I at 405.7 nm and (b) Cr I at 425.4 nm in the soap 1 sample in air at atmospheric pressure.

Figure 3 shows the considerable influence of the delay time upon the LIBS integrated signal intensity. The LIBS signal intensity reaches its maximum value at 720 ns for Pb I and 725 ns for Cr I, representing the optimized delay time for these spectral lines. Furthermore, the impedance of the laser irradiance on the laser plasma generation was studied at various incident laser intensities across the range from 1.0×10^{11} W/cm² to 3.57×10^{11} W/cm². The signal intensities were demonstrated to increase approximately linearly as a function of laser irradiance up to nearly 2.2×10^{11} W/cm² as shown in Figure 4.

Above this value, the increase in the signal intensities was observed to increase in a non-linear fashion. The non-linear behavior may be due to the transition from a thermal to a phase explosive ablation mechanism. Consequently, a laser irradiance of approximately 2.2×10^{11} W/cm² was employed for all subsequent measurements. A representative emission spectrum for the soap 1 sample using the optimized parameters is shown in Figure 5.

The emission spectrum includes a large number of well resolved lines with a low background. The careful examination of this spectrum using the National Institute of Standards and Technology (NIST) atomic spectral database (Ralchenko et al. 2005) revealed the presence of neutral or ionic lines of calcium, neutral lines of aluminum, sodium, iron, and a hydrogen line (H_{α}). Similarly, the prominent spectral lines of toxins, i.e., lead and chromium, may also be observed in the spectrum. The presence of the H_{α} line was due to presence of entrained air from the local environment.

Condition of local thermodynamic equilibrium

To calibrate the LIBS system by using the intensities of the spectral lines, the laser-produced plasma should be thin optically; i.e., the absorption and re-absorption of the incident radiation through the plasma is insignificant. In addition, the plasma should also be in local thermodynamic equilibrium. In a transient system such as a plasma generated for LIBS, the conditions for local thermodynamic equilibrium are attained if the

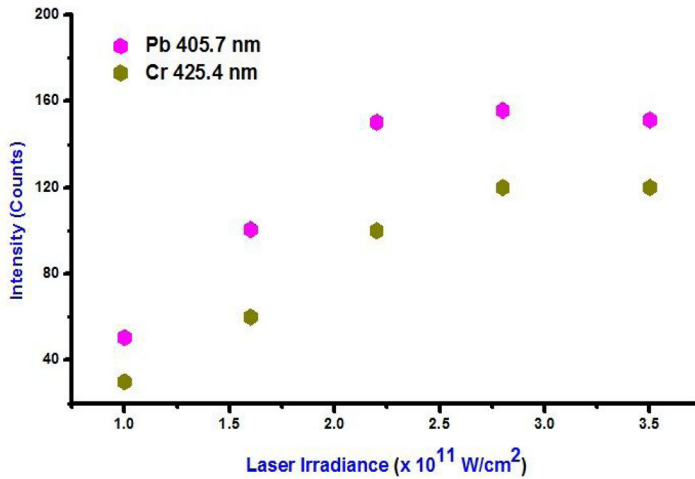


Figure 4. Influence of the laser irradiance upon the LIBS signal for the soap 1 sample in air at atmospheric pressure.

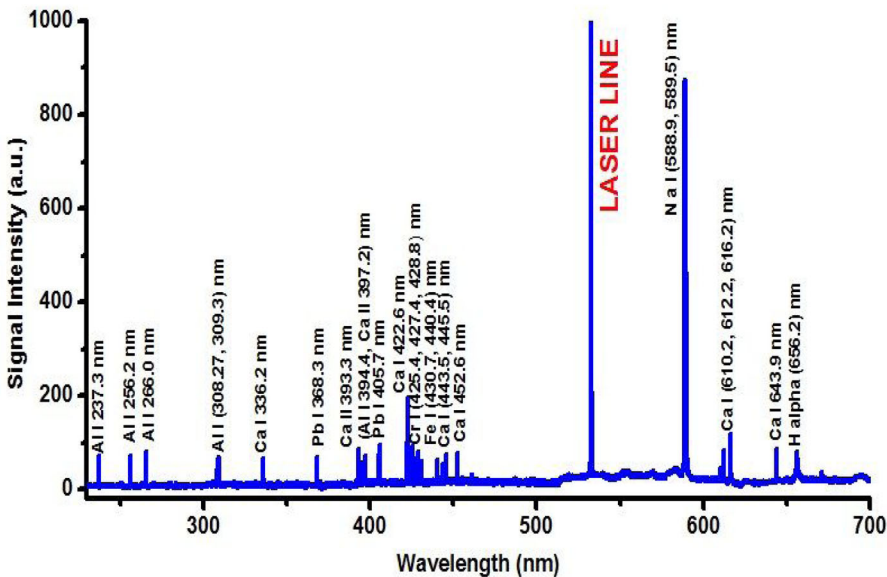


Figure 5. Typical LIBS emission spectrum of the soap 1 sample in air at atmosphere pressure using the 532 nm pulsed Nd:YAG laser.

free electrons in the plasma follow Maxwellian distributions. One should point out that the velocity distribution of the electrons for a comparatively dense plasma at low temperature ($n_e > 10^{16}$ cm⁻³, $kT < 5$ eV) is nearly Maxwellian (Ali et al. 2016; Rehan et al. 2019; Rehan et al. 2016; Rehan et al. 2017).

Additionally, for the conditions of local thermodynamic equilibrium to hold, the collisional, excitation and de-excitation phenomena should be governed by radiative processes. In addition to the plasma boundaries, the number densities are small with rapid movement so that local thermodynamic equilibrium is an unfavorable condition.

However, this assumption is applicable deeper inside the plasma volume where conditions change more gradually and collisions occur more regularly (Harilal et al. 1998). Generally, the conditions of local thermodynamic equilibrium are justified by the McWhirter criterion which states that the electron number density (N_e) must be sufficiently high (Harilal et al. 1998) as described by:

$$N_e \geq 1.6 \times 10^{12} T_e^{1/2} (\Delta E)^3 \quad (1)$$

where N_e is the critical electron density and is dependent upon the energy gap (ΔE) between two adjoining levels of the element considered and T_e is the plasma temperature. In the current study, the Boltzmann plot and Stark broadening line profile methods were used to measure T_e and N_e , respectively. For an optically thin plasma in local thermodynamic equilibrium, the temperature was estimated using the relationship:

$$\ln \left(\frac{I_{ki} \lambda_{ki}}{A_{ki} g_k} \right) = -\frac{E_k}{kT_e} + \ln \left(\frac{N(T_e)}{U(T_e)} \right) \quad (2)$$

where I_{ki} is the intensity of the transition from the upper level (k) to the lower energy level (i), λ_{ki} is the wavelength for the transition, A_{ki} represents the transition probability, g_k is the statistical weight of the upper level (k), $N(T_e)$ is the population of the upper level, $U(T_e)$ is the partition function, E_k is the upper level energy, k is Boltzmann's constant and T_e is the electron temperature.

A straight line was obtained as a result of plotting the variables in Equation (2) resulting in a slope of $-1/kT_e$. The primary causes of uncertainty using equation (2) are the uncertainties in the values of A_{ki} and the integrated intensities as well as the selection of transitions with upper levels having small energy differences (Griem 1997; Rehan et al. 2019). In the current work, T_e was determined by the use of neutral spectral lines of calcium observed in the laser produced plasma for the samples of interest. This selection was made because these spectral lines were well resolved, very intense, and possessed well known transitional probabilities and upper energy levels. A typical Boltzmann plot using the Ca I lines at 336.2 nm, 443.5 nm, 445.5 nm, 452.6 nm, and 643.9 nm for the soap 1 sample is shown in Figure 6.

The electron temperature was determined from the slope of a straight line of Boltzmann plot to be approximately 7850 K. In addition, the value of T_e was also estimated using Al I lines at 256.2 nm, 266.0, 309.3 nm, and 394.4 nm to be approximately 7895 K, thereby providing an average value of 7872 K. In a laser generated plasma, the emission spectral broadening is due to natural broadening, Stark broadening, Doppler broadening, and instrumental broadening. The value of N_e may be estimated by measuring the broadening of a suitable emission line.

In the plasma, atoms are primarily affected by the electric fields induced by adjacent charged particles such as ions and electrons. The atomic energy levels split based on the values of the magnetic quantum number m_j . The coulombic interaction in the plasma is caused by charged particles and radiators. In the LIBS plasma, Stark broadening is caused by neutral and ionized particles. The electrons provide the primary influence due to their higher velocities. The Stark broadening may be related to N_e by

$$\Delta\lambda_{1/2} = 2\omega \left(\frac{N_e}{10^{16}} \right) + 3.5A \left(\frac{N_e}{10^{16}} \right)^{\frac{5}{4}} \left[1 - 1.5ND \frac{-1}{3} \right] \times \omega \quad (3)$$

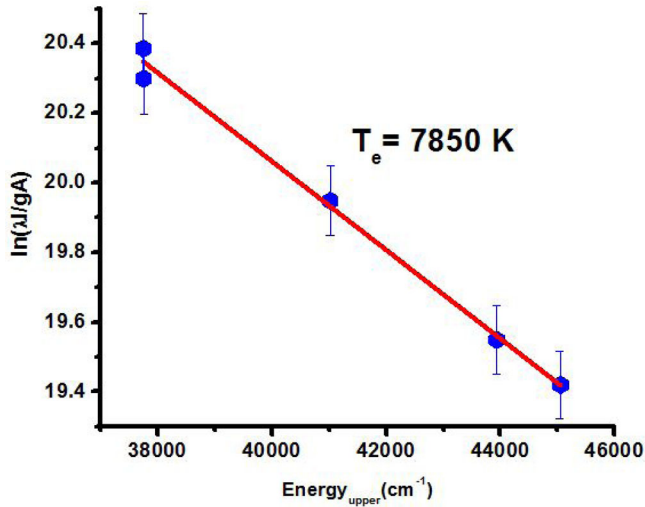


Figure 6. Boltzmann plot using Ca I emission lines for the soap 1 sample in air at atmospheric pressure. Definitions: λ is the wavelength, I is the integrated intensity of the transition, g is the statistical weight, A is the transition probability, and T_e is the plasma temperature.

where $\Delta\lambda_{1/2}$ is the full width at half maximum, ω is for the impact parameter (Dimitrijević & Sahal-Bréchet 1998), A is the ionic broadening, and N_D represents the number of particles in the Debye sphere. The first term in Equation (3) is due to electron broadening while the second term represents the broadening due to ions. As stated above, the contribution from the ionic broadening is insignificant. Therefore the second term may be neglected to give:

$$\Delta\lambda_{1/2} = 2\omega \left(\frac{N_e}{E^{16}} \right) \quad (4)$$

The neutral emission line profile of calcium at 422.67 nm for the $3p^64s4p \ ^1P^0_1 \rightarrow 3p^64s^2 \ ^1S^0$ transition was used to estimate N_e as shown in Figure 7. The solid points represent the measurements that were Lorentzian fitted to provide a value for the full width at half maximum of approximately 0.416 nm. The value of the electron number density for the soap 1 sample using above relationships was estimated to be approximately $3.3 \times 10^{17} \text{ cm}^{-3}$.

The substitution of the value of electron temperature and ΔE for the Ca I line at 422.67 nm allowed the determination of the minimum value of N_e predicted by the McWhirter criteria to be $3.57 \times 10^{15} \text{ cm}^{-3}$, which was smaller than the estimated values. This result implies that the plasma is close to local thermodynamic equilibrium (Rehan et al. 2019). Likewise, McWhirter's criterion was justified for all of the selected samples.

Quantitative study

If the optical length time absorption coefficient is less than 1.0, then the laser induced plasma is said to be optically thin under the conditions of local thermodynamic equilibrium. Under these conditions, the intensity (I) of spectral emission line can be written as (Adrain and Watson 1984):

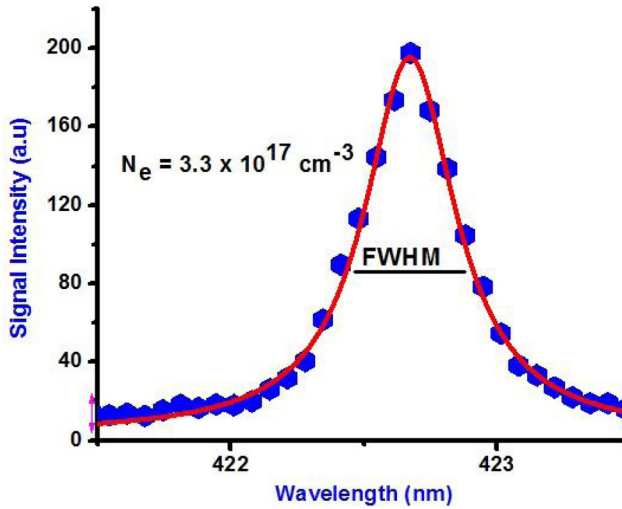


Figure 7. Stark broadened line profile of the Ca I at 422.67 nm for the $3p^64s4p\ ^1P^0_1 \rightarrow 3p^64s^2\ ^1S^0$ transition for the soap 1 sample in air at atmospheric pressure. FWHM is the full width at half maximum and N_e is the electron number density.

$$I = \frac{hcgAN}{4\pi\lambda U} \exp\left(\frac{-\Delta E}{kT_e}\right) \quad (5)$$

where h , c , g , A , N , λ , and Z are Planck's constant, the speed of light, the statistical weight, the Einstein coefficient, the population of ions at ionization state, the wavelength of the selected line, and the partition function, respectively. Similarly, ΔE represents the difference in the energy level, k is Boltzmann's constant and T_e is the plasma temperature. Hence,

$$I \propto N \quad (6)$$

Generally, the quantitative analysis is performed by the construction of calibration curves based on a set of standard samples (usually more than three) with various known abundances of the specific analyte. The calibration curves are obtained by plotting the emission line intensities versus the concentrations of Pb and Cr in the reference samples. These calibration curves were subsequently employed to determine the concentrations of Pb and Cr in the samples.

The calibration standards were prepared by the addition of known concentrations of lead and chromium to the samples. Hence, analyte concentrations equal to 5, 20, 40, 60, and 80 ppm of Pb and Cr were added to the aloe vera based soap and pure aloe vera pulp samples and LIBS spectra were subsequently obtained for these five concentration levels. The spectra of samples were acquired using the optimized LIBS parameters and normalized with the background. The linearity values of the calibration curves were characterized before and after the normalization with the background. The results showed that the linearity of calibration curves was improved using the normalization protocol. Accordingly, the calibration curves after normalization were used for quantitative analysis.

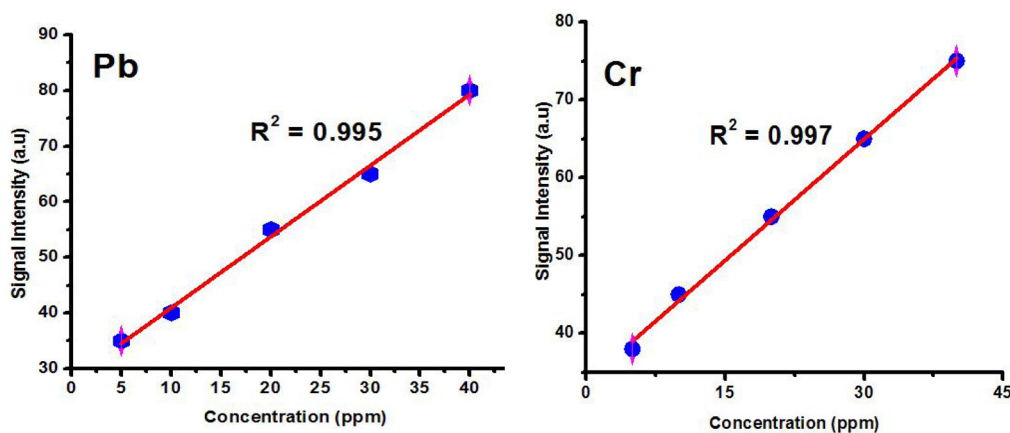


Figure 8. Typical calibration curves for Pb and Cr using the soap 1 sample in air at atmospheric pressure using the Nd:YAG laser at 532 nm.

Typical calibration curves for Pb at 405.7 nm and Cr at 425.4 nm for the soap 1 sample are shown in Figure 8. The figures demonstrate linear increases in the LIBS signal intensity as a function of the concentration. Based upon the calibration curves, the concentrations of Pb and Cr in the aloe vera based beauty soap 1 were determined to be 15.00 and 12.00 ppm, respectively.

The concentrations of lead and chromium estimated by LIBS in each of the samples were further confirmed by ICP-OES measurements that are summarized in Table 1.

The determined concentrations of Pb from 8.00 ppm to 15.00 ppm and Cr from 5.00 to 12.00 ppm were higher than the maximum permissible limits of 0.50 ppm and 1.00 ppm established by the EPA and other regulatory authorities. Surprisingly, the pure aloe vera pulp was contaminated with 14.00 ppm Pb, which is distressingly above the permissible limits and is why its direct use as a cosmetic product is not recommended. The concentration of Cr was below the detection limit of the LIBS system for the pristine aloe vera pulp samples. The highest recorded value of Pb was 15.00 ppm in the soap 1 sample. Based on these obtained results, we suggest that a regular testing program should be implemented to characterize the toxic metals in imported and local cosmetic products to ensure consumer health.

Precision and accuracy of LIBS results

Superior accuracy and precision were obtained by the optimization of the LIBS system. Sufficient warm-up time was provided to allow the laser to stabilize prior to starting the measurements to avoid pulse fluctuations. The statistical errors in the measurements, such as the standard deviation, were minimized by the determination of the average of 20 laser shots for the data acquisition. Also, the spectra were corrected by background subtraction.

The accuracy and precision of the samples by the LIBS and ICP-OES analytical methods are compared in Table 1. The relative accuracy (R.A.) was evaluated as follows:

Table 1. Determination of lead and chromium by laser induced breakdown spectroscopy and inductively coupled plasma in the “test samples” or “pristine alovera and aloe vera based saops” samples. The reported values are provided in parts per million. The measurements were repeated 5 times in air at atmospheric pressure and the average results were found at the 95% confidence limit.

Element	Wavelength (nm)	Sample	Laser induced breakdown spectroscopy	Inductively coupled plasma - optical emission spectroscopy	Standard deviation	Relative Accuracy
Lead	405.7	Soap 1	15.00 ± 0.20	14.10 ± 0.20	0.99	0.07
		Soap 2	09.00 ± 0.20	07.90 ± 0.20	0.80	0.15
		Soap 3	08.00 ± 0.20	08.30 ± 0.20	0.70	0.05
		pulp	14.00 ± 0.30	13.30 ± 0.20	1.12	0.06
chromium	425.4	Soap 1	12.00 ± 0.20	11.20 ± 0.20	0.95	0.08
		Soap 2	05.00 ± 0.10	04.30 ± 0.10	0.89	0.20
		Soap 3	09.00 ± 0.20	08.20 ± 0.20	0.79	0.10
		pulp	Not detected.	Not detected.	Not detected.	Not detected.

$$R.A. = \frac{|d| + S.D. \times \frac{t_{0.975}}{\sqrt{n}}}{M} \quad (7)$$

where d is the difference between the LIBS and the ICP-OES values, S.D. is the standard deviation of LIBS measurements, M is the value from the standard ICP-OES method, n is the number of measurements and $t_{0.975}$ is the Student's t value at 2.5% error confidence. The relative standard deviation (R.S.D.) was determined by:

$$R.S.D. (\%) = \frac{\text{standard deviation } (\sigma_B)}{\text{mean } (n)} \times 100 \quad (8)$$

The relative standard deviation was shown to decrease up to 20 shots. However, no further no improvement in the relative standard deviation was observed with a larger number of laser pulses. The relative standard deviation for the developed LIBS method was approximately 3.4%. The results of selected samples with LIBS were comparable to the values obtained by ICP-OES. As shown in Table 1, the relative accuracy for the LIBS method was in the range from 0.05 to 0.20 which is quite reasonable for reliable analytical measurements.

Conclusion

A laser induced breakdown spectroscopic (LIBS) system was optimized and used to determine the composition of the highly toxic elements Pb and Cr in pure aloe vera pulp and aloe vera based beauty soap. The contents of Pb and Cr determined with the current setup were higher compared to their safe permissible levels. The quantitative determinations were performed by the use of standard calibration curves. The linearity values of the calibration curves were monitored before and after normalization of the spectra with the background. Better results were obtained when the spectrum was normalized by the background.

The concentrations of Pb and Cr determined with the LIBS system were verified using a standard ICP-OES protocol. The values obtained by the two techniques were closely matched. Moreover, the relative accuracy values of the LIBS system for lead and

chromium were in the range from 0.05 to 0.20 at 2.5% error confidence. The present study will not only add to the existing literature but also provide important information for the health of aloe-vera based cosmetics users.

Disclosure statement

There are no conflicts of interest to declare.

References

- Adrain, R., and J. Watson. 1984. Laser microspectral analysis: A review of principles and applications. *Journal of Physics D: Applied Physics* 17 (10):1915–40. doi: [10.1088/0022-3727/17/10/004](https://doi.org/10.1088/0022-3727/17/10/004).
- Al-Saleh, I. 1998. Sources of lead in Saudi Arabia: A review. *Journal of Environmental Pathology, Toxicology and Oncology: Official Organ of the International Society for Environmental Toxicology and Cancer* 17 (1):17–35.
- Al-Saleh, I., S. Al-Enazi, and N. Shinwari. 2009. Assessment of lead in cosmetic products. *Regulatory Toxicology and Pharmacology* 54 (2):105–13. doi: [10.1016/j.yrtph.2009.02.005](https://doi.org/10.1016/j.yrtph.2009.02.005).
- Ali, A., M. Khan, I. Rehan, K. Rehan, and R. Muhammad. 2016. Quantitative classification of quartz by laser induced breakdown spectroscopy in conjunction with discriminant function analysis. *Journal of Spectroscopy* 2016:1–6. doi: [10.1155/2016/1835027](https://doi.org/10.1155/2016/1835027).
- Baral, A., and R. D. Engelken. 2002. Chromium-based regulations and greening in metal finishing industries in the USA. *Environmental Science & Policy* 5 (2):121–33. doi: [10.1016/S1462-9011\(02\)00028-X](https://doi.org/10.1016/S1462-9011(02)00028-X).
- Dimitrijević, M. S., and S. Sahal-Bréchet. 1999. Stark broadening of neutral calcium spectral lines. *Astronomy and Astrophysics Supplement Series* 140 (2):191–2. doi: [10.1051/aas:1999416](https://doi.org/10.1051/aas:1999416).
- Augusto, D. S., A. Batista, and É. F. Pereira-Filho. 2016. Direct chemical inspection of eye shadow and lipstick solid samples using laser-induced breakdown spectroscopy (LIBS) and chemometrics: Proposition of classification models. *Analytical Methods* 8 (29):5851–60. doi: [10.1039/C6AY01138A](https://doi.org/10.1039/C6AY01138A).
- Gondal, M., Y. Maganda, M. Dastageer, F. Al-Adel, A. Naqvi, and T. Qahtan. 2013. Development of a laser induced breakdown sensor for detection of carcinogenic chemicals in cosmetic products. *IEEE 2013 High Capacity Optical Networks and Emerging/Enabling Technologies*, 84–7.
- Gondal, M., Z. Seddigi, M. Nasr, and B. Gondal. 2010. Spectroscopic detection of health hazardous contaminants in lipstick using laser induced breakdown spectroscopy. *Journal of Hazardous Materials* 175 (1-3):726–32. doi: [10.1016/j.jhazmat.2009.10.069](https://doi.org/10.1016/j.jhazmat.2009.10.069).
- Griem, H. 1997. *Principles of plasma spectroscopy*. Cambridge: Cambridge University.
- Harilal, S., C. Bindhu, V. Nampoori, and C. Vallabhan. 1998. Temporal and spatial behavior of electron density and temperature in a laser-produced plasma from $\text{YBa}_2\text{Cu}_3\text{O}_7$. *Applied Spectroscopy* 52 (3):449–55. doi: [10.1366/0003702981943671](https://doi.org/10.1366/0003702981943671).
- Hepp, N. M., W. R. Mindak, and J. Cheng. 2009. Determination of total lead in lipstick: Development and validation of a microwave-assisted digestion, inductively coupled plasma-mass spectrometric method. *Journal of Cosmetic Science* 60:405–14.
- Lambers, H., S. Piessens, A. Bloem, H. Pronk, and P. Finkel. 2006. Natural skin surface pH is on average below 5, which is beneficial for its resident flora. *International Journal of Cosmetic Science* 28 (5):359–70. doi: [10.1111/j.1467-2494.2006.00344.x](https://doi.org/10.1111/j.1467-2494.2006.00344.x).
- Lorentz, L. J., A. M. Api, L. Babcock, L. M. Barraja, J. Burdick, K. C. Cater, G. Jarrett, S. Mann, Y. H. L. Pan, T. A. Re, et al. 2008. Exposure data for cosmetic products: Facial cleanser, hair conditioner, and eye shadow. *Food and Chemical Toxicology* 46 (5):1516–24. doi: [10.1016/j.fct.2007.12.011](https://doi.org/10.1016/j.fct.2007.12.011).
- Luo, W., D. Ruan, C. Yan, S. Yin, and J. Chen. 2012. Effects of chronic lead exposure on functions of nervous system in Chinese children and developmental rats. *Neurotoxicology* 33 (4): 862–71. doi: [10.1016/j.neuro.2012.03.008](https://doi.org/10.1016/j.neuro.2012.03.008).

- Nohynek, G. J., E. Antignac, T. Re, and H. Toutain. 2010. Safety assessment of personal care products/cosmetics and their ingredients. *Toxicology and Applied Pharmacology* 243 (2): 239–59. doi: [10.1016/j.taap.2009.12.001](https://doi.org/10.1016/j.taap.2009.12.001).
- Ralchenko, Y., F. C. Jou, D. E. Kelleher, A. Kramida, A. Musgrove, J. Reader, W. L. Wiese, and K. J. Olsen. 2005. NIST Atomic Spectra Database (version 3.0). <http://physics.nist.gov/asd3>.
- Rehan, I., M. A. Khan, R. Muhammad, M. Khan, A. Hafeez, A. Nadeem, and K. Rehan. 2019. Operational and Spectral Characteristics of a Sr–Ne Glow Discharge Plasma. *Arabian Journal for Science and Engineering* 44 (1):561–8. doi: [10.1007/s13369-018-3439-0](https://doi.org/10.1007/s13369-018-3439-0).
- Rehan, I., M. Z. Khan, K. Rehan, S. Abrar, Z. Farooq, S. Sultana, N. U. Saqib, and H. Anwar. 2018. Optimized laser-induced breakdown spectroscopy for the determination of high toxic lead in edible colors. *Applied Optics* 57 (21):6033–9. doi: [10.1364/AO.57.006033](https://doi.org/10.1364/AO.57.006033).
- Rehan, I., K. Rehan, S. Sultana, M. O. Ul Haq, M. Z. K. Niazi, and R. Muhammad. 2016. Spatial characterization of red and white skin potatoes using nano-second laser induced breakdown in air. *The European Physical Journal Applied Physics* 73 (1):10701–9. doi: [10.1051/epjap/2015150453](https://doi.org/10.1051/epjap/2015150453).
- Rehan, K., I. Rehan, S. Sultana, M. Z. Khan, Z. Farooq, A. Mateen, and M. Humayun. 2017. 2017. Determination of Metals Present in Textile Dyes Using Laser-Induced Breakdown Spectroscopy and Cross-Validation Using Inductively Coupled Plasma/Atomic Emission Spectroscopy. *International Journal of Spectroscopy* 2017:1–9. doi: [10.1155/2017/1614654](https://doi.org/10.1155/2017/1614654).
- Renfrew, M. M. 1991. NIOSH Pocket guide to chemical hazards (US Department of Health and Human Services-National Institute for Occupational Safety and Health). ACS Publications.
- Saeed, M., N. Muhammad, and H. Khan. 2011. Assessment of heavy metal content of branded Pakistani herbal products. *Tropical Journal of Pharmaceutical Research* 10 (4):499–506. doi: [10.4314/tjpr.v10i4.16](https://doi.org/10.4314/tjpr.v10i4.16).
- Tomankova, K., K. Kejlova, S. Binder, A. Daskova, J. Zapletalova, H. Bendova, H. Kolarova, and D. Jirova. 2011. In vitro cytotoxicity and phototoxicity study of cosmetics colorants. *Toxicology in Vitro* 25 (6):1242–50. doi: [10.1016/j.tiv.2011.04.026](https://doi.org/10.1016/j.tiv.2011.04.026).
- Vigeh, M., H. Saito, and S-i Sawada. 2011. Lead exposure in female workers who are pregnant or of childbearing age. *Industrial Health* 49 (2):255–61. doi: [10.2486/indhealth.MS1192](https://doi.org/10.2486/indhealth.MS1192).
- Wilding, B. C., K. Curtis, and L. K. Welker-Hood. 2009. Hazardous chemicals in health care. Physicians for Social Responsibility.